Electronic Supplementary Material (ESI) for Journal of Materials Chemistry C.

Supplementary Material

Design, synthesis and application of tetraphenylbenzene-based blue organic electroluminescent materials with aggregation-induced emission and hot exciton properties

Xiaorui Dong[a#], Yinpeng Cao[a#], Xiuqing Dong[a*], Jinnan Huo[a,b*], Heping Shi[a*]

[a]School of Chemistry and Chemical Engineering, Shanxi University, Taiyuan 030006, China.

[b]School of Pharmacy, Liaoning University of Traditional Chinese Medicine, Dalian 116600, China.

*** Correspondence:**

Corresponding Author

Heping Shi, E-mail address: hepingshi@sxu.edu.cn

Jinnan Huo, E-mail address: 15364911443@163.com

Xiuqing Dong, E-mail address: dongxq@sxu.edu.cn

[#]Xiaorui Dong and Yinpeng Cao have equal contribution

1. Common measurements and characterization

^1H NMR and ^{13}C NMR spectra were recorded on Bruker Amx 600 MHz/Bruker Dex 400 MHz instrument using deuterated chloroform as solvents. Molecular masses were measured on matrix-assisted laser desorption ionization time-of-flight high-resolution mass spectrometer (MALDI-TOF-HRMS). Ultraviolet-visible absorption spectra were obtained on a Shimadzu UV-2450 and fluorescence spectroscopy were measured on a Shimadzu RF-5301PC. Thermogravimetric analysis (TGA) and differential scanning calorimetry (DSC) were carried out on TGA 2050 thermogravimetric analyzer and DSC 2910 modulated calorimeter under the protection of nitrogen at a heating rate of 10°C min^{-1}, respectively. Cyclic voltammetry (CV) was performed on a CHI-600 electrochemical workstation with tetrabutylammonium hexafluorophosphate (0.1 M) in acetonitrile as electrolyte, platinum electrode as the working electrode, Ag/AgCl as the reference electrode, and platinum wire as the auxiliary electrode. Transient PL decay were recorded on an Edinburgh Instruments FLS920.

2. Device fabrication and measurements

Doped and non-doped OLEDs with the configurations of ITO/HATCN (10 nm)/TAPC (50 nm)/Emitter (x wy%): DPEPO (20 nm)/TmPyPB (40 nm)/LiF (1 nm)/Al (100 nm) were prepared using **TPB-CN-CZ1** and **TPB-CN-CZ2** as emitters by vacuum-deposition at 200°C. The light-emitting layer materials were purified by sublimation before being used in device preparation. All devices are prepared on indium tin oxide (ITO) conductive glass plates. Before preparing the devices, the ITO substrate was cleaned in an ultrasonic instrument, then dried for 2 h, and finally pretreated with oxygen plasma for 4 min. Then the organics were vapor-deposited onto the ITO film in a vacuum (p<5×10^{-5} Pa) vapor deposition chamber. The deposition rates of organic materials, LiF and Al were controlled at 1-2 Å/s, 0.1 Å/s, and 6 Å/s, respectively. The electroluminescence spectra were recorded on a Hitachi MPF-4 fluorescence spectrometer. The current density-voltage characteristics of the OLEDs were measured on a Keithley 2400 source meter. Using the combination of 3645 DC power and 1980A spot photometer to test the current density-voltage-luminance curves.

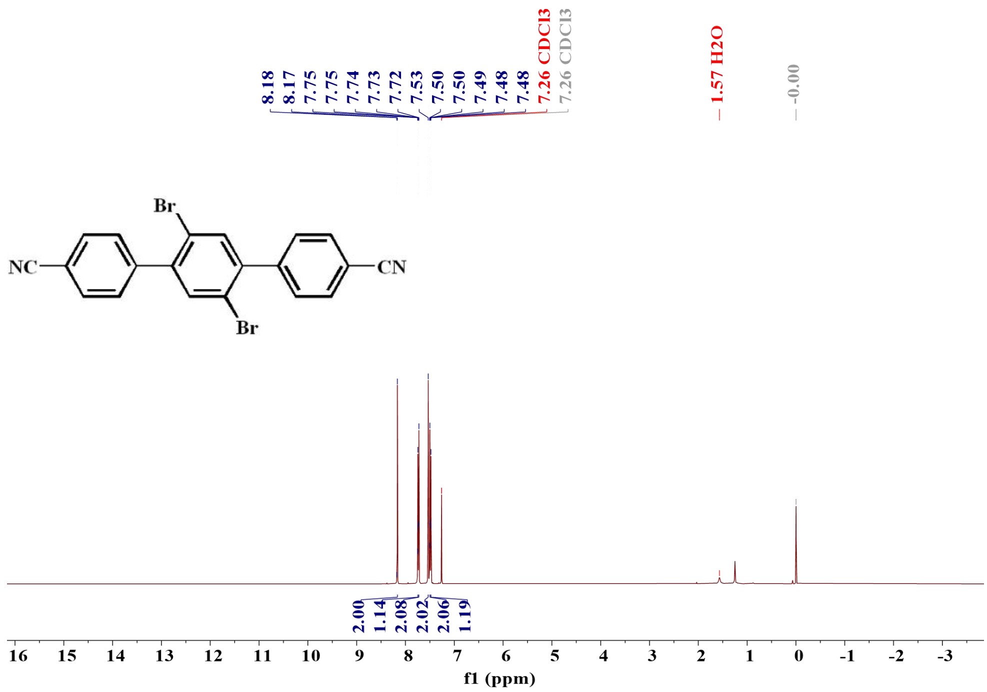

^{1}H NMR of compound C1

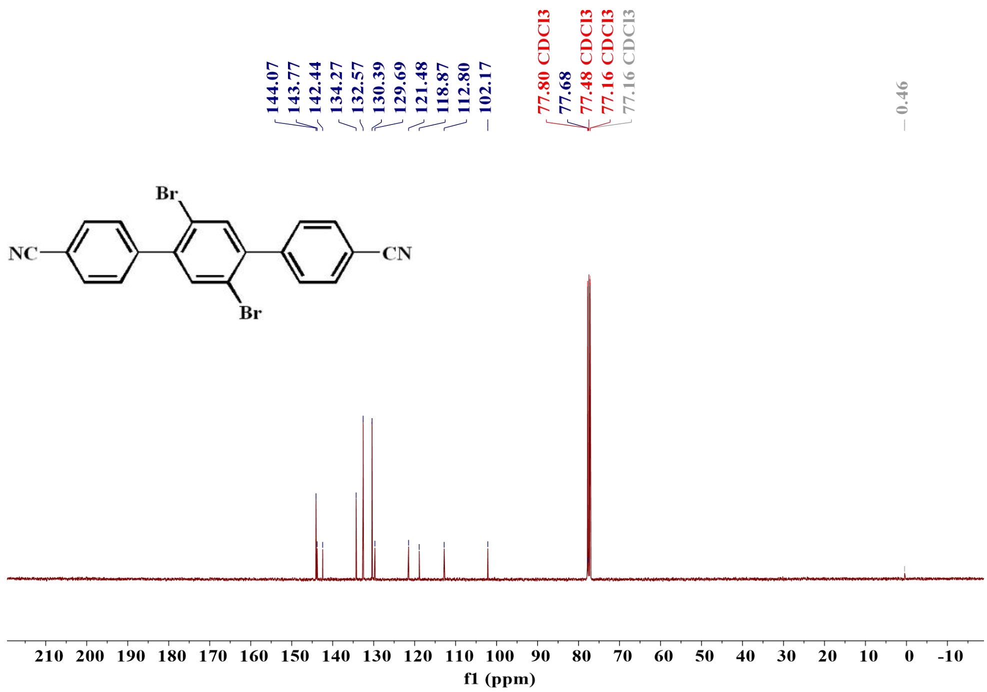

^{13}C NMR of compound C1

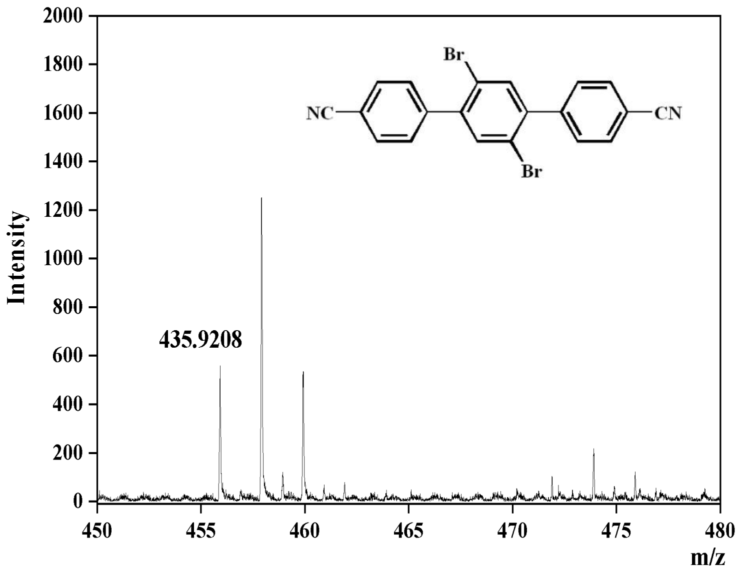

MS of compound C1

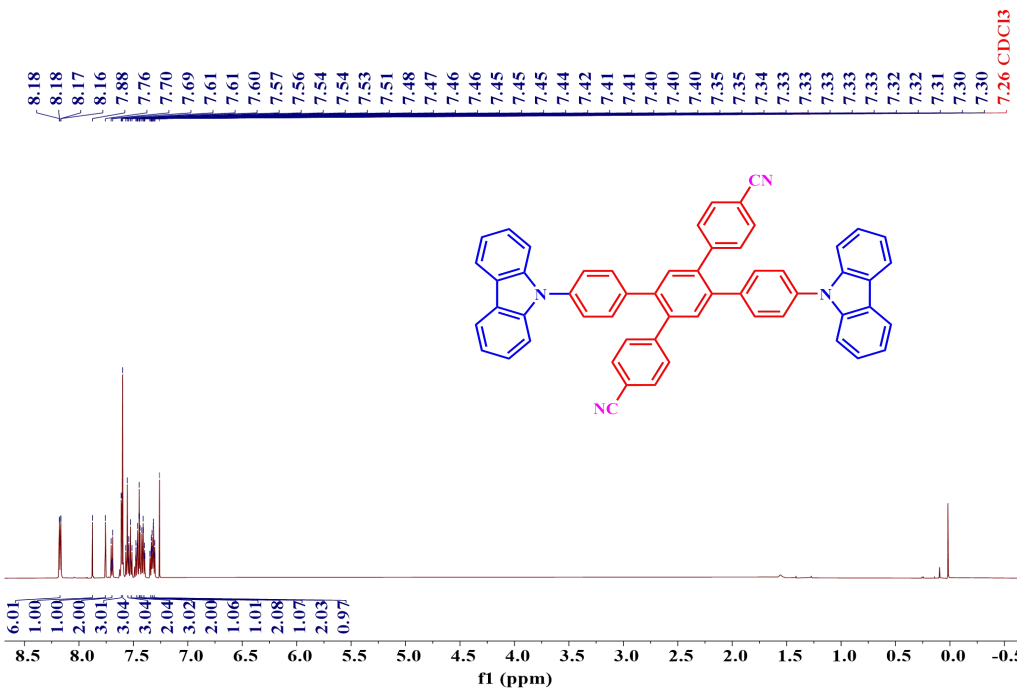

^{1}H NMR of **TPB-CN-CZ1**

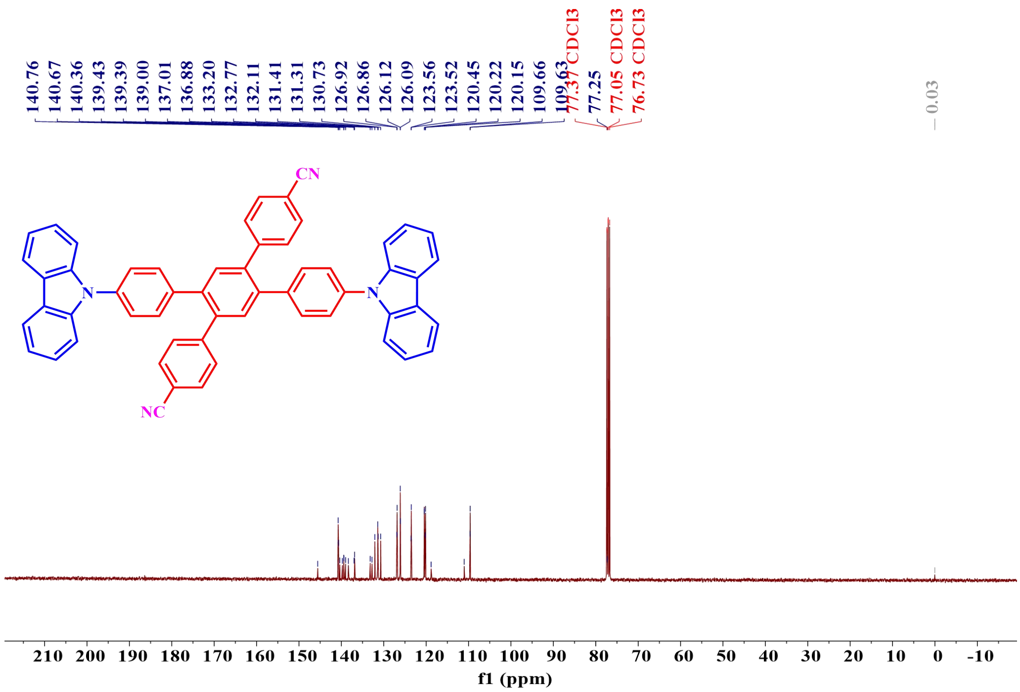

^{13}C NMR of **TPB-CN-CZ1**

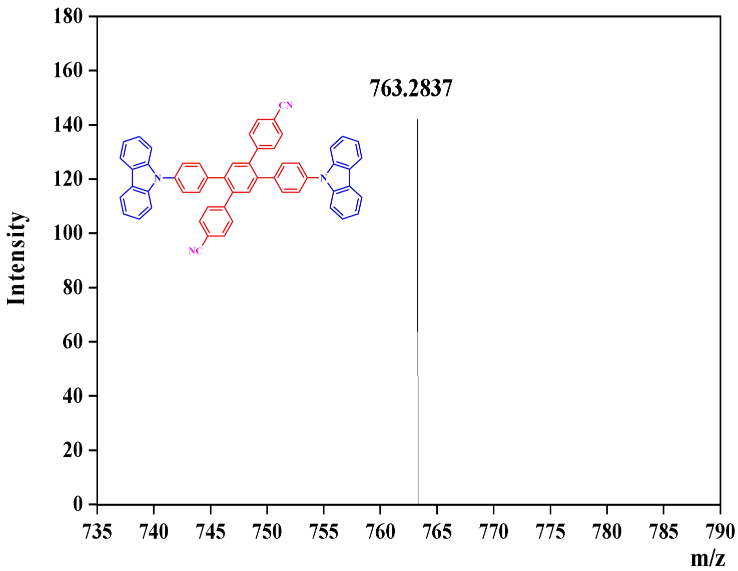

MS of **TPB-CN-CZ1**

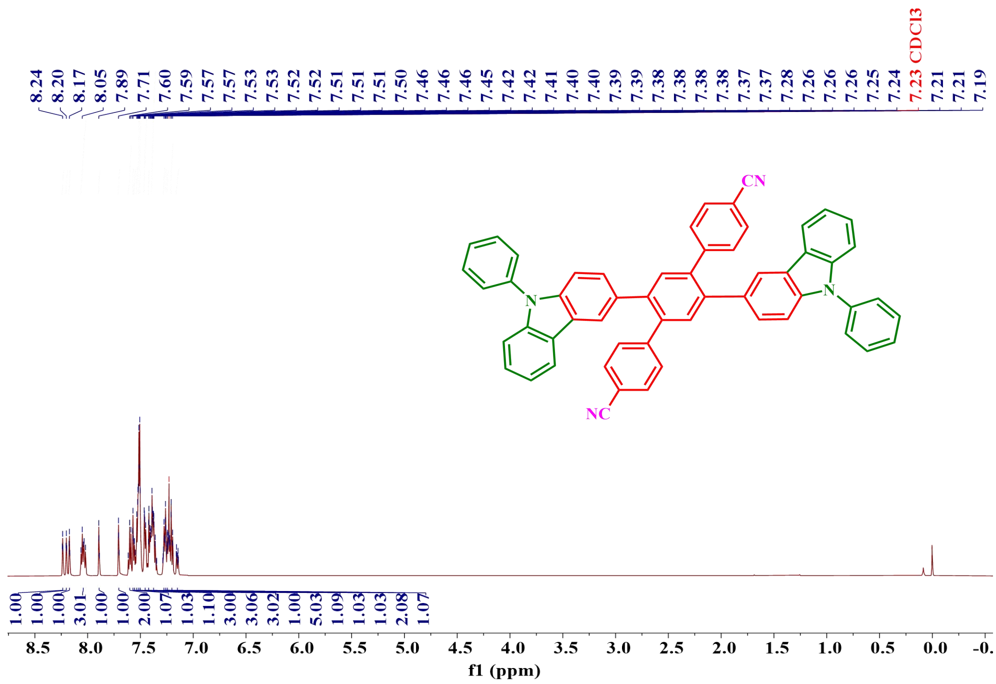

^{1}H NMR of **TPB-CN-CZ2**

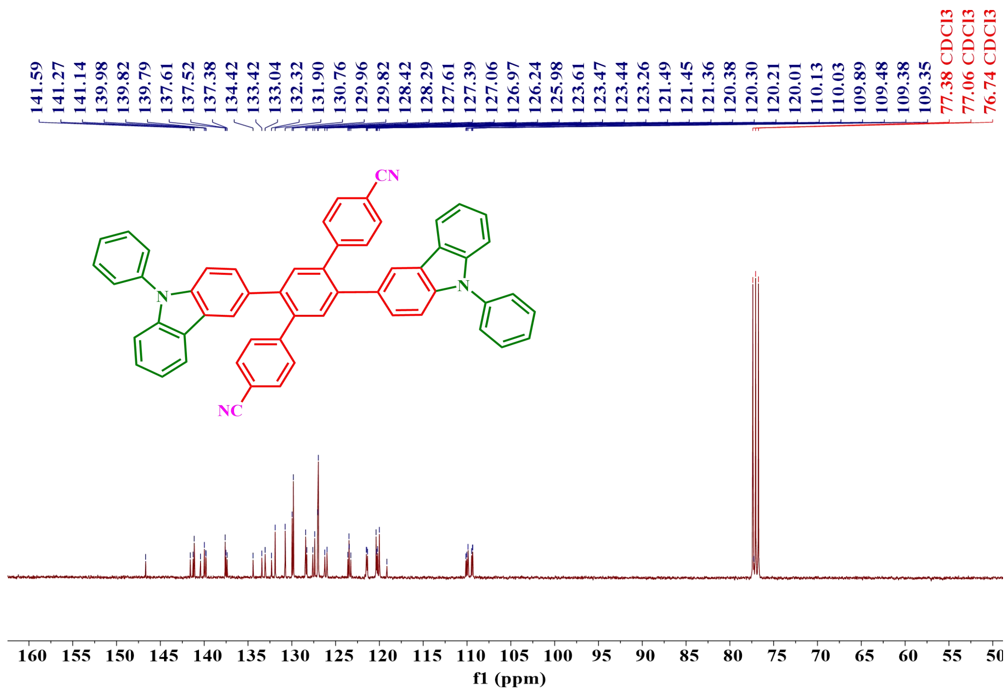

^{13}C NMR of **TPB-CN-CZ2**

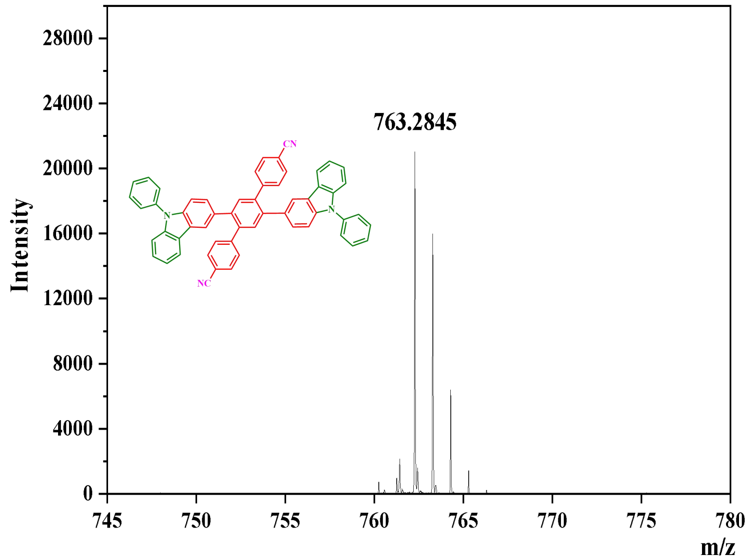

MS of **TPB-CN-CZ2**

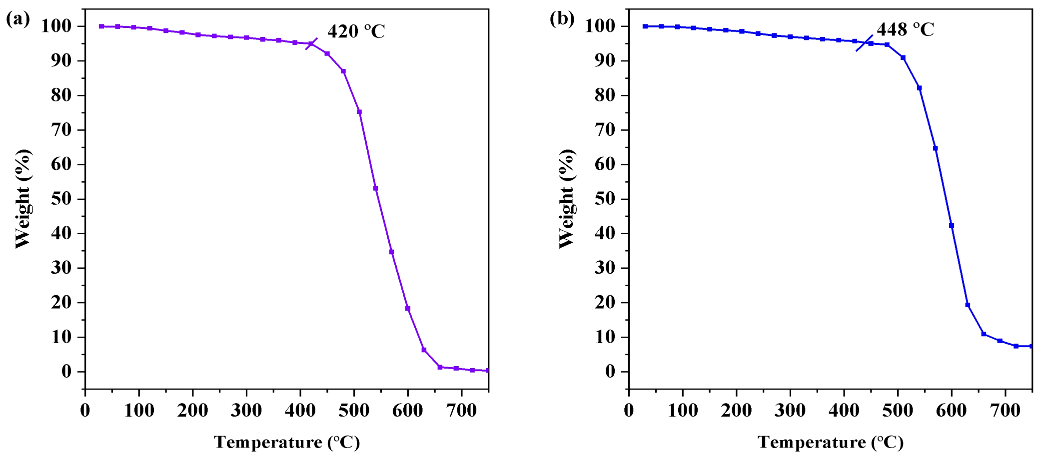

Fig. S1 TGA curves of (a) **TPB-CN-CZ1** and (b) **TPB-CN-CZ2**.

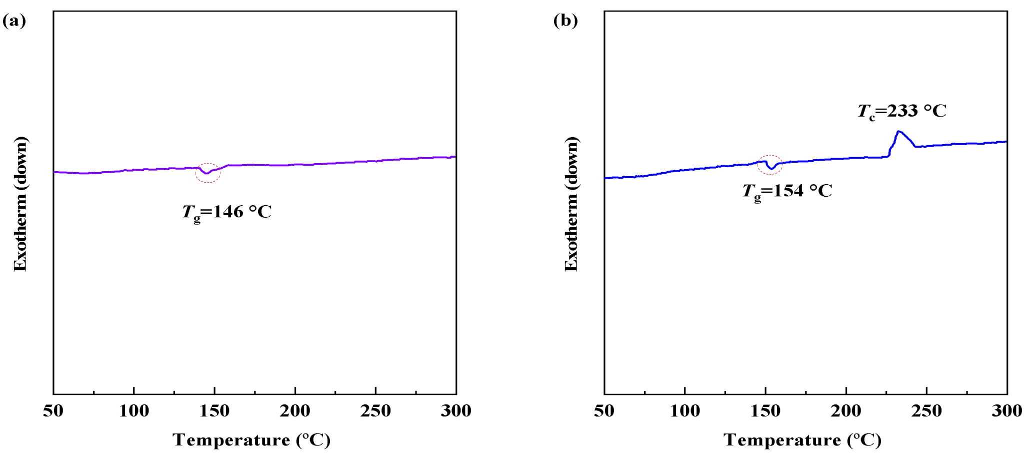

Fig. S2 DSC curves of (a) **TPB-CN-CZ1** and (b) **TPB-CN-CZ2**.

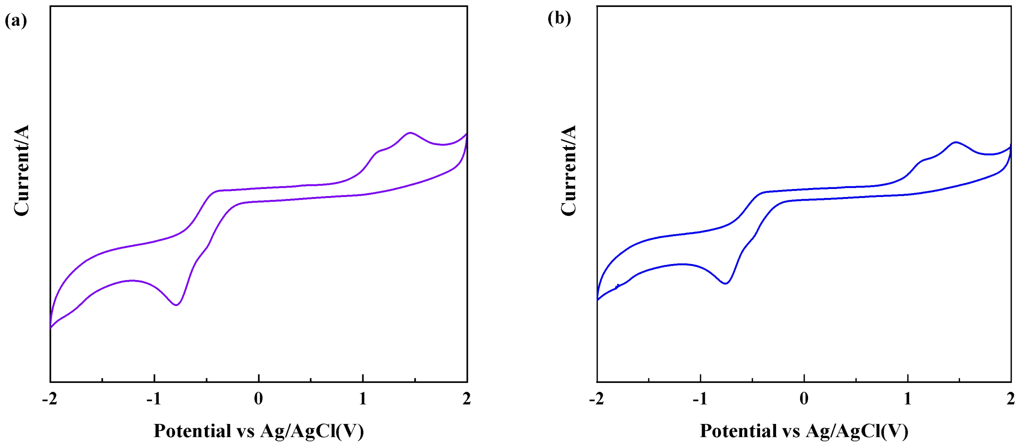

Fig.S3 CV curves of (a) **TPB-CN-CZ1** and (b) **TPB-CN-CZ2**.

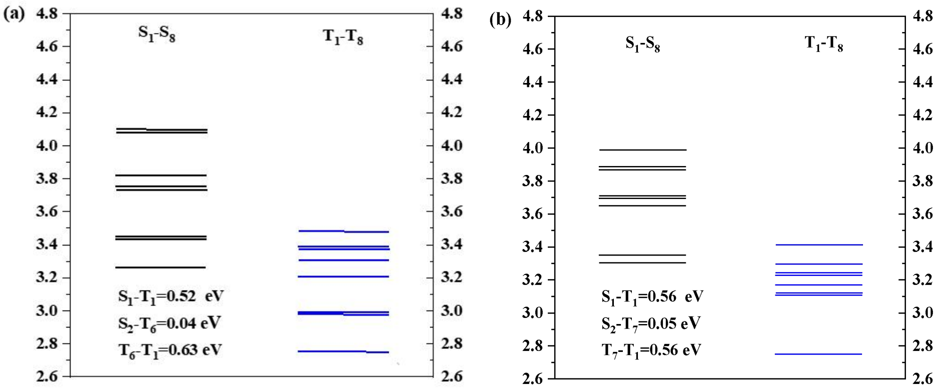

Fig. S4 Energy level distribution of vertical excitation energy for (a) **TPB-CN-CZ1** and (b) **TPB-CN-CZ2**.

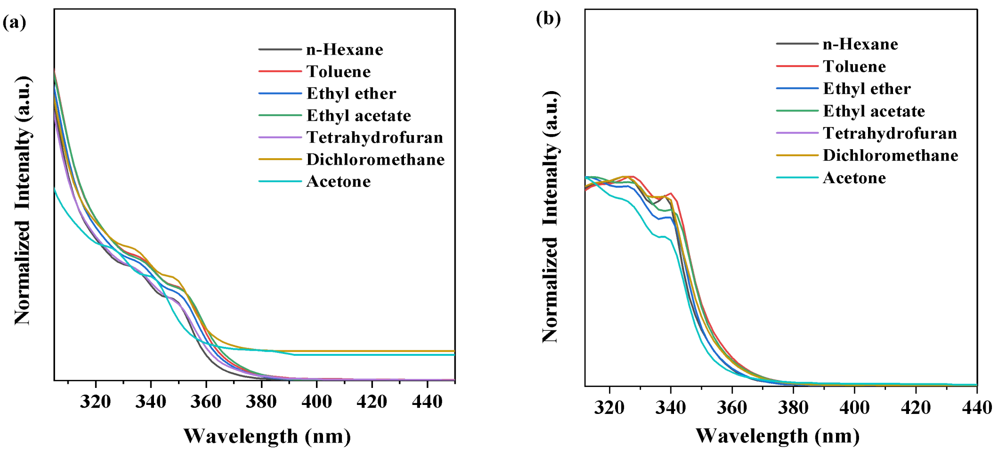

Fig. S5 UV-vis absorption spectra in different solvents of (a) **TPB-CN-CZ1** and (b) **TPB-CN-CZ2**.

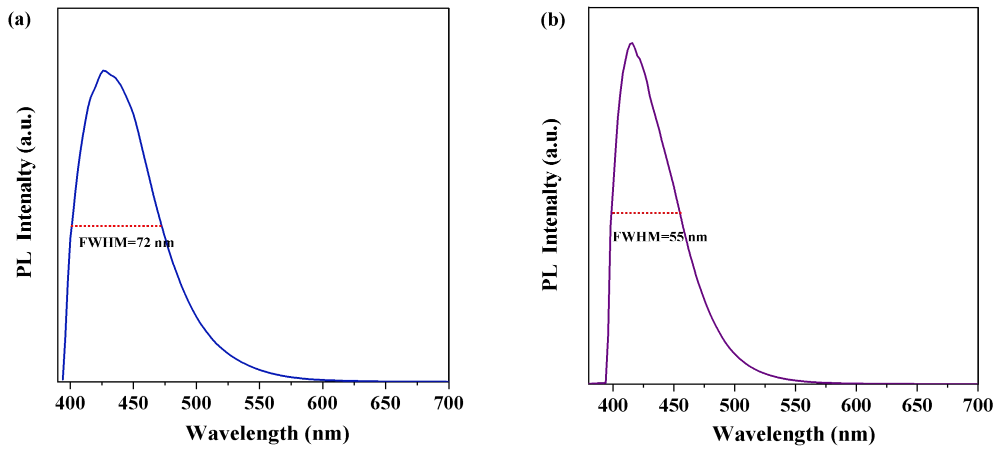

Fig. S6 PL spectra in film of (a) **TPB-CN-CZ1** and (b) **TPB-CN-CZ2**.

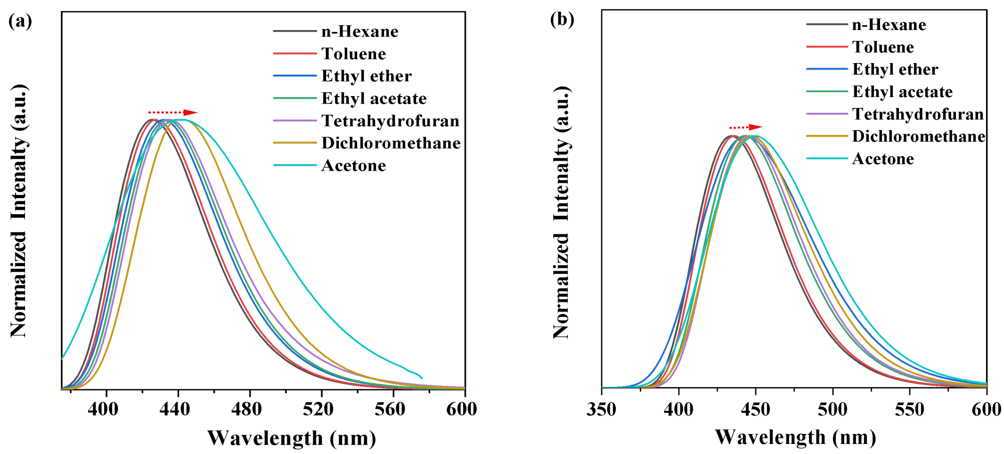

Fig. S7 PL spectra in different solvents of (a) **TPB-CN-CZ1** and (b) **TPB-CN-CZ2**.

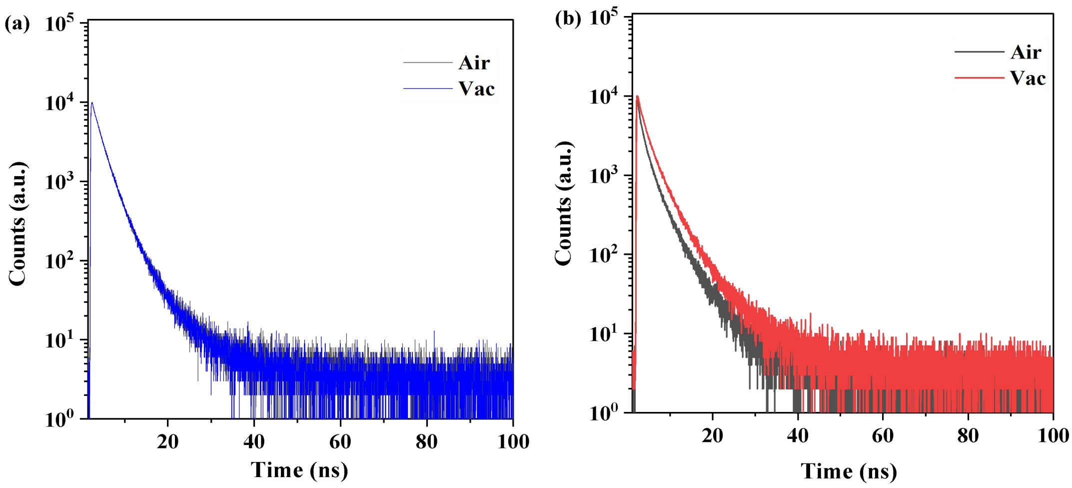

Fig. S8 Transient PL spectra of (a) **TPB-CN-CZ1** and (b) **TPB-CN-CZ2**.

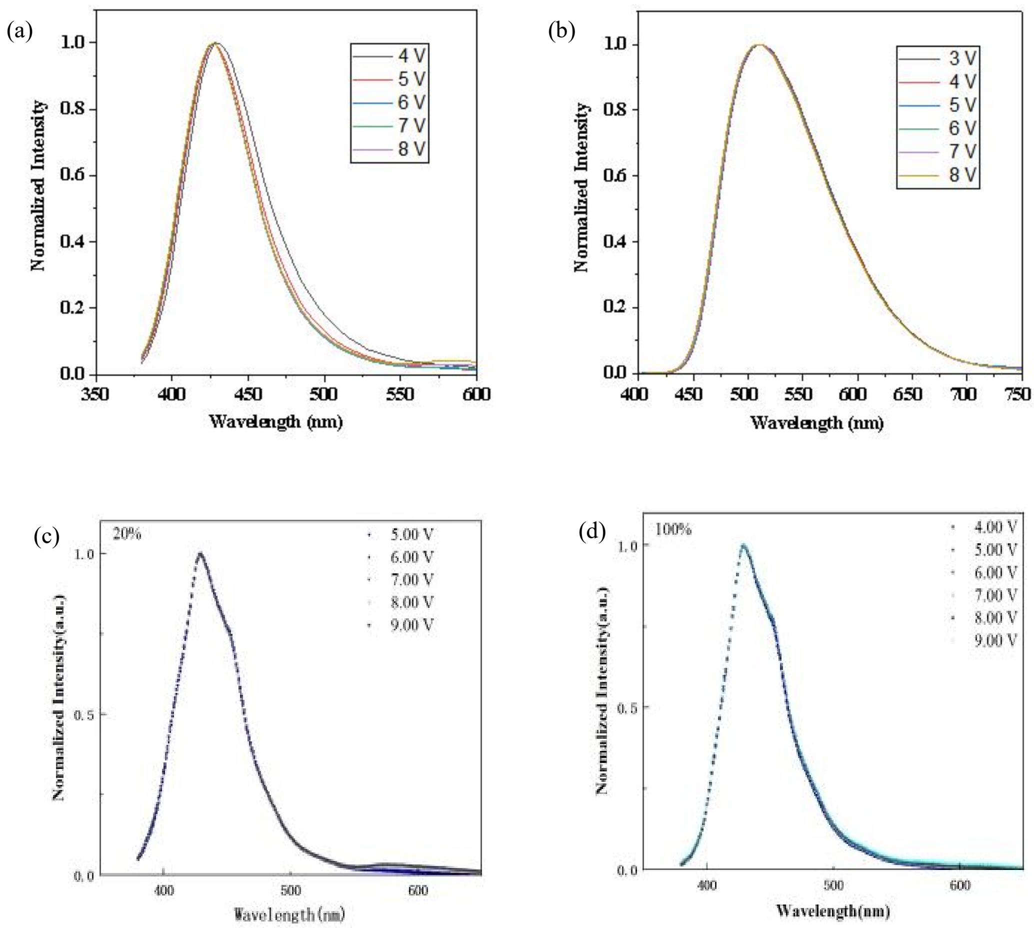

Fig. S9 EL spectra of device (a) A, (b) B, (c) M and (d) N.

Table S1 Nature transition orbitals and properties of $S_0 \rightarrow S_n$ (n=1-8) for **TPB-CN-CZ1**

	Transition Character	**Hole**	**Particle**	**Contribution**	**Δr**
$S_0 \rightarrow S_1$	LE	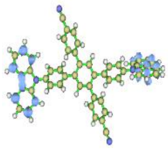	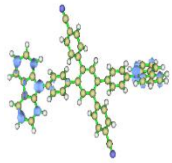	98.4%	1.2 Å
$S_0 \rightarrow S_2$	CT	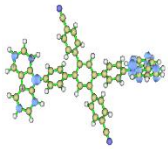	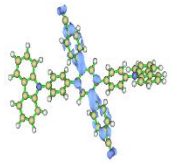	98.6%	5.6 Å
$S_0 \rightarrow S_3$	CT	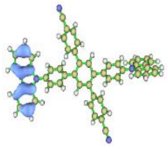	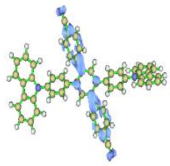	99.0%	5.9Å
$S_0 \rightarrow S_4$	CT	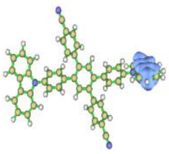	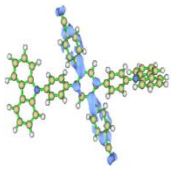	99.0%	5.9Å
$S_0 \rightarrow S_5$	CT	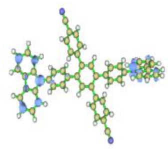	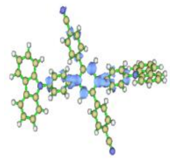	94.7%	4.3Å
$S_0 \rightarrow S_6$	CT	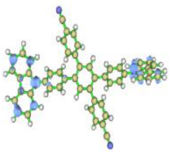	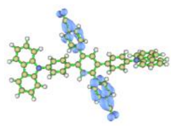	98.2%	4.4Å
$S_0 \rightarrow S_7$	CT	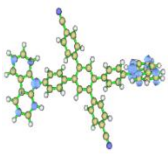	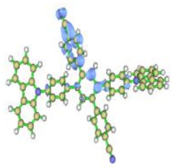	96.5%	4.7Å
$S_0 \rightarrow S_8$	CT	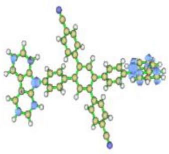	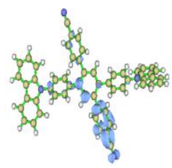	97.2%	4.5Å

Table S2 Nature transition orbitals and properties of $S_0 \rightarrow T_n$ (n=1-8) for **TPB-CN-CZ1**

	Transition Character	**Hole**	**Particle**	**Contribution**	**Δr**
$S_0 \rightarrow T_1$	HLCT	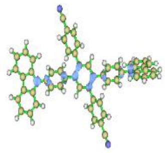	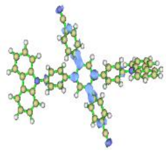	80.1%	3.3Å
$S_0 \rightarrow T_2$	CT	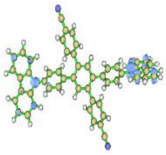	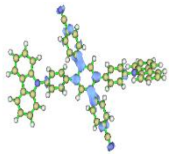	88.2%	4.2Å
$S_0 \rightarrow T_3$	HLCT	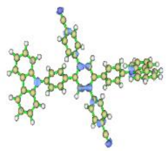	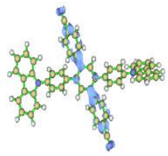	75.2%	2.9Å
$S_0 \rightarrow T_4$	LE	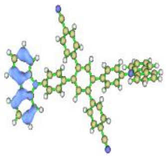	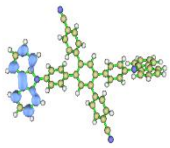	75.1%	1.4Å
$S_0 \rightarrow T_5$	HLCT	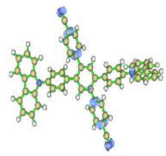	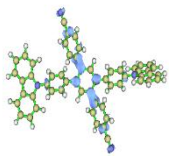	76.2%	2.7Å
$S_0 \rightarrow T_6$	CT	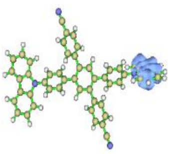	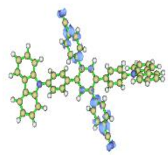	60.3%	4.2Å
$S_0 \rightarrow T_7$	HLCT	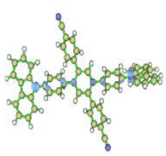	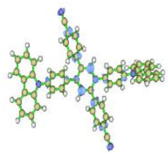	34.5%	3.2Å
$S_0 \rightarrow T_8$	CT	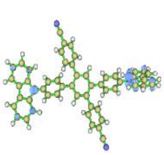	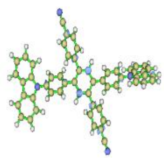	52.0%	4.6Å

Table S3 Nature transition orbitals and properties of $S_0 \rightarrow S_n$ (n=1-8) for **TPB-CN-CZ2**

	Transition Character	Hole	Particle	Contribution	Δr
$S_0 \rightarrow S_1$	LE	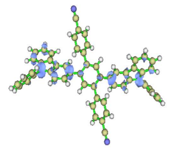	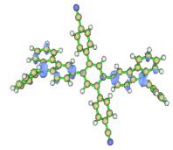	98.4%	1.7 Å
$S_0 \rightarrow S_2$	CT	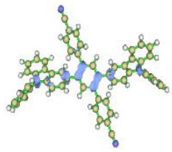	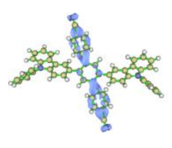	98.6%	3.4 Å
$S_0 \rightarrow S_3$	CT	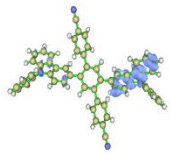	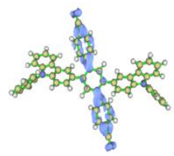	99.0%	3.9Å
$S_0 \rightarrow S_4$	CT	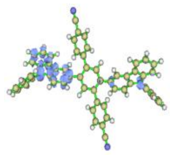	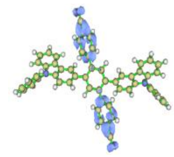	99.0%	4.2Å
$S_0 \rightarrow S_5$	CT	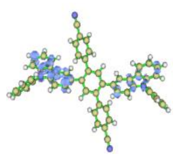	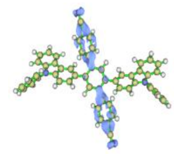	94.7%	4.1Å
$S_0 \rightarrow S_6$	LE	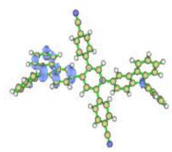	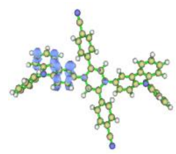	98.2%	2.4Å
$S_0 \rightarrow S_7$	CT	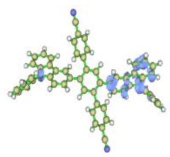	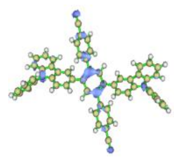	96.5%	4.2Å
$S_0 \rightarrow S_8$	CT	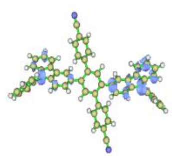	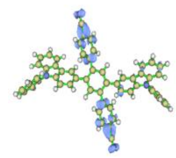	97.2%	4.0Å

Table S4 Nature transition orbitals and properties of $S_0 \rightarrow T_n$ (n=1-8) for **TPB-CN-CZ2**

	Transition Character	**Hole**	**Particle**	**Contribution**	**Δr**
$S_0 \rightarrow T_1$	LE	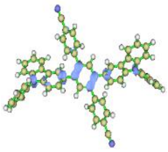	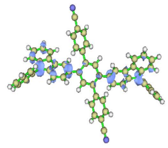	80.1%	2.7Å
$S_0 \rightarrow T_2$	CT	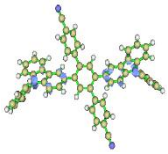	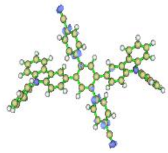	88.2%	4.2Å
$S_0 \rightarrow T_3$	LE	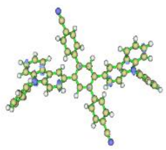	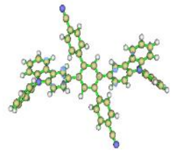	75.2%	1.8Å
$S_0 \rightarrow T_4$	LE	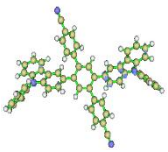	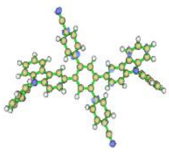	75.1%	1.4Å
$S_0 \rightarrow T_5$	CT	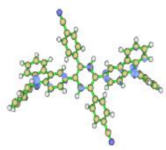	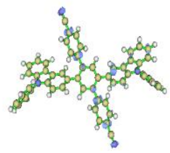	76.2%	4.4Å
$S_0 \rightarrow T_6$	CT	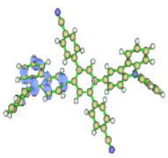	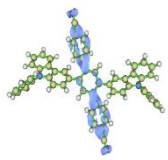	60.3%	4.0Å
$S_0 \rightarrow T_7$	HLCT	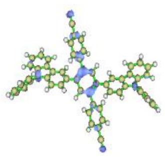	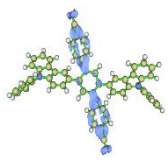	34.5%	2.9Å
$S_0 \rightarrow T_8$	CT	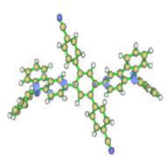	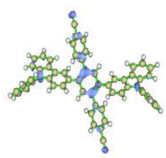	52.0%	4.6Å

Table S5 Photophysical properties of **TPB-CN-CZ1** in different solvents

Solvent	n-Hexane	toluene	ethyl ether	ethyl acetate	tetrahydrofuran	dichloromethane	acetone
λ_{abs}	350	350	352	352	350	348	354
λ_{em}	426	428	432	434	436	438	440
Stokes shift (cm^{-1})	5097	5206	5260	5367	5635	5904	5521
PLQY (%)	5.6	6.9	11.8	12.3	20.9	20.9	21.7

Table S6 Photophysical properties of **TPB-CN-C2** in different solvents

Solvent	n-Hexane	toluene	ethyl ether	ethyl acetate	Tetrahydrofuran	dichloromethane	acetone
λ_{abs}	338	340	340	340	342	340	340
λ_{em}	434	436	444	442	446	448	450
Stokes shift (cm^{-1})	6544	6476	6889	6787	6818	7090	7189
PLQY (%)	8.7	9.6	11.4	13.0	13.2	12.6	18.8